Controlling cell destruction using dielectrophoretic forces

A. Menachery and R. Pethig

Abstract: Measurements are reported of the main factors, namely the AC voltage frequency and magnitude, that were observed to influence the number of cells destroyed during dielectrophoresis (DEP) experiments on Jurkat T cells and HL60 leukemia cells. Microelectrodes of interdigitated and quadrupolar geometries were used. A field-frequency window has been identified that should be either avoided or utilised, depending on whether or not cell damage is to be minimised or is a desired objective. The width and location of this frequency window depends on the cell type, as defined by cell size, morphology and dielectric properties, and is bounded by two characteristic frequencies. These frequencies are the DEP cross-over frequency, where a cell makes the transition from negative to positive DEP, and a frequency determined by the time constant that controls the frequency dependence of the field induced across the cell membrane. When operating in this frequency window, and for the microelectrode designs used in this work, cell destruction can be minimised by ensuring that cells are not directed by positive DEP to electrode edges where fields exceeding 30–40 kV/m are generated. Alternatively, this field-frequency window can be exploited to selectively destroy specific cell types in a cell mixture.

1 Introduction

The possibility that, under certain conditions, cells may be irreversibly damaged as a result of exposure to dielectrophoresis (DEP) forces is well known to workers in the field, but is often not reported. The desired objective in many DEP experiments is to use radio-frequency electric fields to selectively isolate, concentrate, or purify target bioparticles from prepared or natural fluid suspensions. Examples include the isolation of cancer cells, fetal cells, stem cells or bacteria from blood for further analysis or potential therapeutic purposes. Maintaining cell viability is an important objective in such cases. For some of our previous studies, the frequency and voltage of the applied electrical signals were programmed to avoid regimes where cell damage had been observed [1]. For other envisaged applications of DEP, as for example to facilitate the release of proteins or DNA from target cells, utilising such frequency-voltage regimes to achieve selective cell destruction may be a desired objective.

DEP-induced cell damage can arise from at least three main sources: (i) effects associated with the cells being suspended in a non-physiological medium; (ii) stress induced by the applied electric field; and (iii) shear stresses associated with fluid flow. Workers in the field are now competent in their choice of cell suspending media and applied signal voltages, so that under gentle DEP conditions cell viability can be readily maintained. For example, the viability of erythrocytes separated from leukemia cells has been verified using trypan blue dye [2] and CD34+ cells have been successfully cultured following their DEP enrichment from bone marrow and peripheral stem cell harvests [3]. Fibroblasts can be successfully cultivated, without significant change in their viability, motility, anchorage or cell-cycle time, when exposed to DEP fields continuously over a period of 3 days [4]. Although very small increases were observed in the stress-related gene c-fos expression levels for glioma and neuroblastoma cells separated by DEP, subsequent culturing experiments demonstrated that there were no effects on cell growth [5]. The highest reported fluid flow rate for DEP cell separation appears to be 2.5 ml/min [6]. Because of the relatively small dimensions of a typical DEP separation chamber, this flow rate is well within the limits for laminar flow and corresponds to a shear stress exerted on the cells of around 0.3 N/m^2. This is well below the shear stress of 150 N/m^2 required to damage erythrocytes [7] or of 20 N/m^2 for T cells [8].

Cell membranes can also be disrupted by forced oscillation at frequencies greater than around 10 kHz, and this is the basis for using high-power sonication to disintegrate cells. Cell destruction by DEP is more subtle, and is primarily related to a field-induced breakdown of the physical integrity of the plasma membrane, as evidenced by the fact that the internal structure of the cell appears (under phase-contrast microscopy) to remain intact for some time and is even manipulable by DEP [9]. A related topic is electroporation (also called electropermeabilisation) of cells, which is typically achieved by subjecting cells to electric pulses of field strengths ranging from around 5 MV/m (for microsecond pulses) down to 0.1 MV/m (for millisecond pulses) [10]. Field-frequency maps have also been produced of the observed probability of AC electromediated cell bursting [11].

We now intend to analyse the conditions, in terms of the strength and frequency of the applied AC field, under which two different cell types (human T cells and HL60 leukemia cells) can be observed to burst during routine DEP

IEE Proceedings online no. 20050010

doi:10.1049/ip-nbt:20050010

Paper received 24th May 2005

The authors are with the School of Informatics, University of Wales, Bangor, Dean Street, Bangor, Gwynedd, LL57 1UT, UK

E-mail: ron@informatics.bangor.ac.uk

experiments. This analysis will provide insights into the main factors that can be controlled to either minimise or to achieve selected cell destruction using dielectrophoresis.

2 Theory

As described in standard texts e.g. [12] the total force, per unit volume, acting on a dielectric particle subjected to an external electric field E is given by:

$$F_v = \rho E - \frac{\varepsilon_o}{2} E^2 \nabla \varepsilon_r + \frac{\varepsilon_o}{2} \nabla \left(E^2 \frac{d\varepsilon_r}{dg} g \right) \quad (1)$$

In this equation, ρ represents the net charge density carried by the particle, ε_0 is the permittivity of free space, ε_r and g are the relative permittivity and density of the particle material, respectively, and ∇ is the grad vector operator. The first term of (1) is thus the electrophoretic force acting on a charged particle, whereas the second term is a force that will appear if the particle is composed of a dielectrically inhomogeneous material. The last term gives a volume force in an inhomogeneous electric field and hence represents the DEP force [13], where the factor $d\varepsilon_r/dg$ is given by the Clausius-Mossotti relationship that $(\varepsilon_r - 1)/(\varepsilon_o + 2)$ should be proportional to the density of the material [14].

A rigorous way to apply (1) utilises the Maxwell stress tensor to determine the time-averaged mechanical forces and torques (tensions acting along field lines and pressures acting perpendicular to them) exerted by an electric field on the surface and within the body of a particle [12, 15]. This method involves determining difficult integrals that incorporate pressure-like variables that are difficult to test experimentally, so that for most practical applications the Maxwell stress tensor formulation is not 'user friendly'. The so-called 'effective dipole' method gives the same results as the more rigorous Maxwell stress tensor method, and has the advantage that it uses simple concepts and relatively straightforward analyses [16]. Based on this theory the time-averaged DEP force, acting on a homogeneous spherical particle of radius R suspended in a medium of relative permittivity ε_m, is given by:

$$\langle F_{DEP} \rangle = 2\pi \varepsilon_o \varepsilon_m R^3 \mathrm{Re}[f(\varepsilon^*)] \nabla |E|^2 \quad (2)$$

where E is the root-mean-squared amplitude of the applied AC field. $\mathrm{Re}[f(\varepsilon^*)]$ is the real part of the Clausius-Mossotti factor:

$$f(\varepsilon^*) = \left(\frac{\varepsilon_c^* - \varepsilon_e^*}{\varepsilon_c^* + 2\varepsilon_e^*} \right) \quad (3)$$

and is bounded by the values $-0.5 \leq \mathrm{Re}[f(\varepsilon^*)] \leq 1.0$. Positive values signify a positive DEP (cells attracted to high-field regions at electrode edges) and negative values give a negative DEP (cells repelled from electrode edges). The factors ε_c^* and ε_e^* are the cell and extracellular medium complex permittivities, respectively, defined by $\varepsilon^* = \varepsilon - j(\sigma/\omega)$ with ε being the permittivity, σ the conductivity, ω the radian frequency $(2\pi f)$ and $j = \sqrt{-1}$.

To obtain a significant DEP force, the factor $\nabla |E|^2$ in (2) should be of the order of 10^{13} V^2/m^3, which, depending on the electrode geometry, can correspond to an applied field of the order of 10 kV/m or lower [17]. The reason a relatively weak DEP field can cause electrical damage to a cell is because the field is 'amplified' in the form of a potential induced across the cell membrane. For a model, spherical, cell the frequency dependence of the field E_m acting across the membrane is given by [18, 19] and references cited therein as:

$$E_m(\omega, \theta) = \frac{1.5(R/d)E\cos\theta}{1 + j\omega\tau} \quad (4)$$

The factor R/d is the ratio of the cell radius R to the membrane thickness d ($\sim$5 nm) and θ is the polar angle with respect to the field direction. The time constant τ is given by:

$$\tau = RC_m \Big/ \left(\frac{2\sigma_i\sigma_e}{\sigma_i + 2\sigma_e} + \frac{R}{d}\sigma_m \right) \quad (5)$$

where σ_i, σ_m, and σ_e are the conductivities of the cell interior (cytoplasm), cell membrane and extracellular medium, respectively. C_m is the membrane capacitance whose value is principally determined by the morphology of the cell in terms of the presence of microvilli, blebs or membrane folds, for example, and to a good approximation can be determined experimentally from the expression [20]:

$$C_m = \frac{\sqrt{2}}{2\pi R f_{xo}} \sigma_e \quad (6)$$

In this equation, f_{xo} is the frequency (the so-called DEP cross-over frequency) where the cell exhibits a transition from negative to positive DEP. Equation (4) predicts that at low frequencies $(\omega\tau < 1)$ the field E_m acting across a cell membrane can exceed the applied field E by a factor of 10^3 or greater, depending on cell size.

3 Experimental

3.1 Cell samples

Human T lymphocytes (Jurkat E6-1) and leukemia cells (HL60) were obtained from the American Type Culture Collection (ATCC: TIB-152) and the European Collection of Cell Cultures (ECACC: 85011431), respectively. The T cells were grown in RPMI media containing modified RPMI-1640 (ATCC) supplemented with 10% fetal bovine serum (ATCC), 100 U/ml penicillin, and 100 µg/ml streptomycin (Gibco/BRL). The HL60 cells were grown in RPMI-1640 media (Sigma) supplemented with 10% fetal bovine serum (Sigma), 1 mM glutamine and 20 mM hepes buffer (Sigma). A humidified incubator was used, and maintained at 37°C, with 5% CO_2, 95% air.

Immediately before the DEP experiments, the cells were washed twice with 10 ml of an isotonic low conductivity media containing 8.6% w/w sucrose, 0.3% w/w dextrose, and 1.0 mg/ml BSA (Sigma), pH 7.4. The conductivity of this media was adjusted to 40 mS/m at 25°C, by adding modified Eagle's minimum essential media (Sigma) at a ratio of about 40:1, and using a YSI 3200 conductivity instrument with an Orion 018012 conductivity flow cell. After washing, the cells were suspended in the 40 mS/m media. The osmolality of the cell suspensions remained near 296 mmol/kg, as determined using a Vapro 5520 vapour pressure osmometer. The osmolality and conductivity of the cell suspensions were checked before and after each DEP experiment.

3.2 Dielectrophoresis and cell bursting observations

Two microelectrode designs were employed in the experiments, namely the interdigitated-castellated and quadrupolar (polynomial) geometries shown in Fig. 1. The interdigitated electrodes were fabricated with a characteristic dimension of 80 µm defining the castellation geometry [21], and for the quadrupole design [22] the distance between opposing electrode tips was 400 µm. The electrode material was gold, 70 nm thick, vacuum evaporated onto a

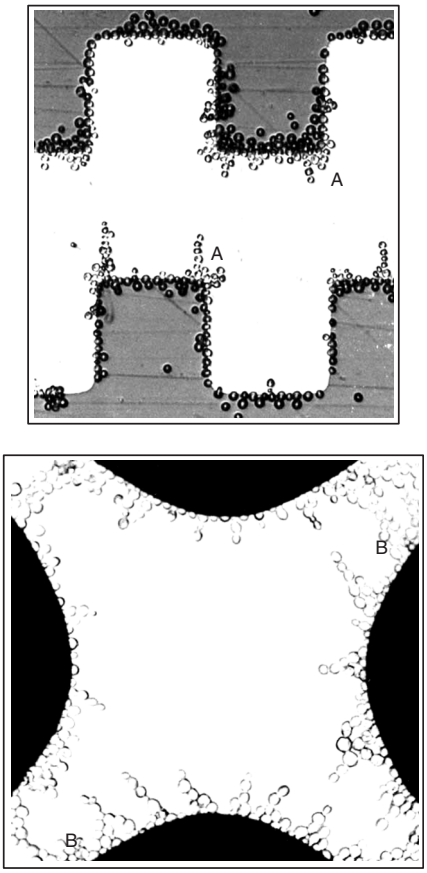

Fig. 1 *The interdigitated and quadrupole electrodes used in these studies are shown on the top and bottom, respectively. The characteristic dimension defining the interdigitated castellations was 80 μm, and the distance between opposing quadrupole electrode tips was 400 μm. Cells are shown being attracted to the electrode edges under the influence of positive DEP, cell bursts events were most common in regions such as those marked A and B*

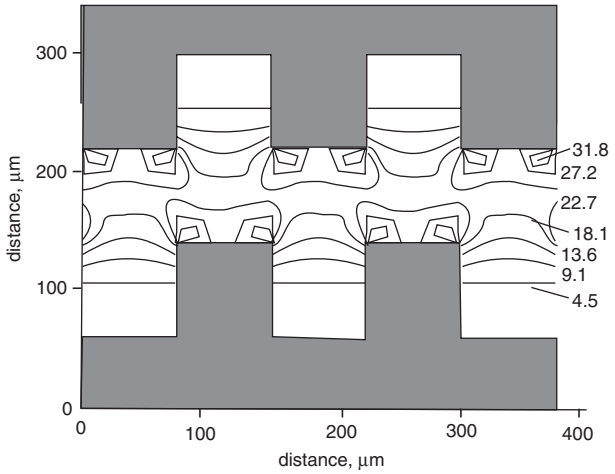

Fig. 2 *The electric field contours (in kilovolts per metre) generated by the interdigitated electrodes with an applied sinusoidal AC voltage of 1 V (peak)*

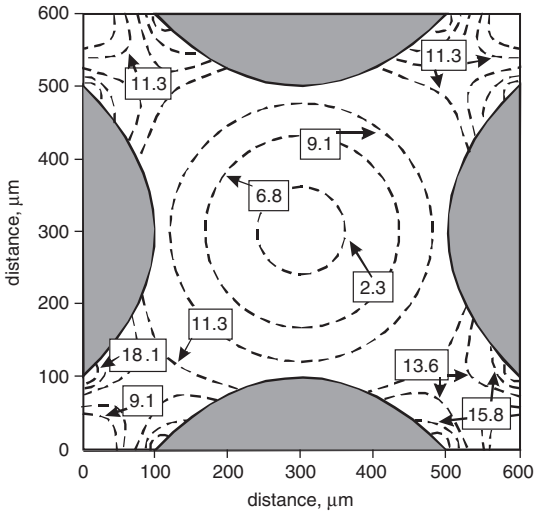

Fig. 3 *The field contours (in kilovolts per metre) generated by the quadrupolar electrodes with an applied sinusoidal AC voltage of 1 V (peak)*

5 nm thick seed layer of chromium on a glass microscope slide substrate. Further details of these electrode designs, their fabrication, and how they are used for DEP experiments, have been given elsewhere [21, 22].

The data collected for cell bursting events were obtained during experiments performed primarily to characterise the DEP properties of T cells and HL60 cells. The results obtained for the T cells have been reported elsewhere [20] and during the course of these experiments approximately 5% of the cells burst on approaching the (polynomial design) electrode edges under the influence of a positive DEP force. In these experiments the location of each cell could be continuously tracked, and a value for the diameter of each cell could be determined to within $\pm 0.25\,\mu m$ [20]. The observations made of the location of the cells when they burst, and of the magnitude and frequency of the applied AC voltages, constitute the bulk of the data presented in this study. Cell bursting events for a smaller number of T cells were also observed using the interdigitated electrode geometry. The data collected for the HL60 cells were all made using interdigitated electrodes, and in these experiments the locations of the cells and their diameters ($\pm 0.5\,\mu m$) were determined using a simple video imaging method. Cell bursting was observed to occur most often (but not always) in the inter-electrode regions marked 'A' and 'B' in Fig. 1, for the interdigitated and quadrupolar electrodes, respectively.

The magnitudes of the local electric fields imposed on the cells at the time of their observed bursting were deduced from field contour maps of the form shown in Figs. 2 and 3. These maps were obtained using the Femlab Electromagnetics Module (COMSOL, Inc.) in conjunction with the Matlab (The Math Works, Inc.) environment, for a 1 V peak sinusoidal signal applied to the electrodes, and as a function of height (up to 15 μm) above the electrode plane. Most of the experiments were performed with an applied AC sinusoidal voltage in the range 2–6 V (peak), and simple linear scalings of the contours given in Figs. 2 and 3 were adopted to accommodate these different voltages. One experiment was performed to induce increased numbers of HL60 cell bursting events, by increasing the interdigitated electrode voltage up to 12 V (peak).

4 Results

The cell bursting events, in terms of the local fields experienced by the cells and the frequencies of the applied voltages, are shown in Fig. 4. HL60 cell bursting events for the experiments where the voltage was increased up to 12 V (peak) are not included in this Figure (but see Fig. 6). The data points for the HL60 and T cells can be seen to fall into

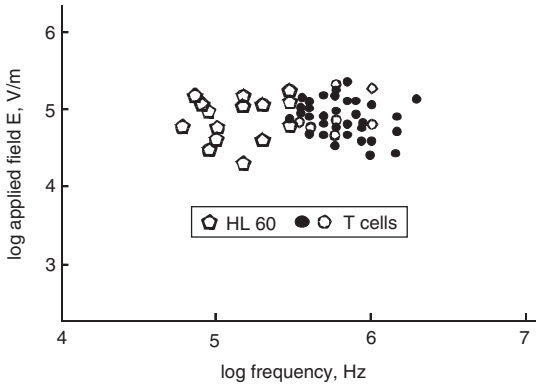

Fig. 4 *Values of the local field and voltage signal frequency at which HL60 and T cells were observed to burst in a suspending electrolyte of conductivity 40 mS/m. The HL60 data points were obtained using the interdigitated electrode design. Both quadrupole (filled circles) and interdigitated (open circles) electrodes were used for the T cell studies*

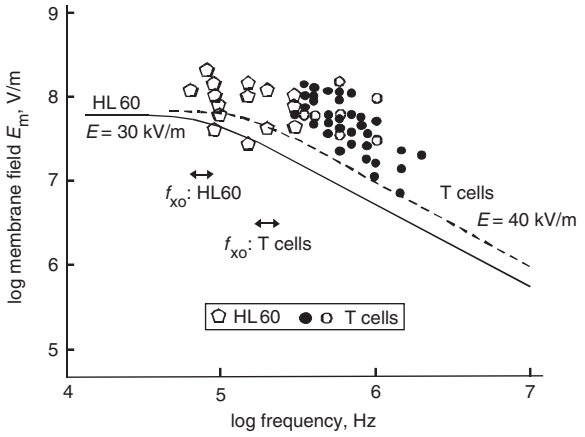

Fig. 5 *Values obtained from (4), using the field-frequency data given in Fig. 4, for the induced field membrane at the time of cell bursting. Also shown are the DEP cross-over (f_{xo}) frequency range values measured for the HL60 and T cells that did not burst. The solid curve shows how the membrane field varies with frequency for the HL60 cells for an applied local field of 30 kV/m and a suspending medium conductivity of 40 mS/m. The dotted line gives the same information for T cells in a local field of 40 kV/m*

fairly distinct field-frequency windows. The fact that the results obtained for the T cells did not depend on whether polynomial or interdigitated electrodes were employed indicates that difference in cell type, rather than choice of electrode geometry, determined the different experimental parameters observed for cell bursting.

The data of Fig. 4 has been used to produce Fig. 5, to show values of the membrane field generated parallel to the applied field (i.e. $\theta = 0$) in each cell at the instant of their bursting. These calculations employed (4) and required the value of the cell radius (which was measured in the experiments) as well as the membrane capacitance C_m to determine the time constant τ given by (5). For the T cells, the value for C_m was taken as the average value 13.24 mF/m^2 determined in [20] for the large number (>600) of cells that did not burst during the experiments. In (5) the experimental value of 40 mS/m was used for the conductivity σ_e of the external suspending medium, and values of 0.7 S/m and 5×10^{-7} S/m were assumed for the conductivities σ_i and σ_m of the cell interior and membrane,

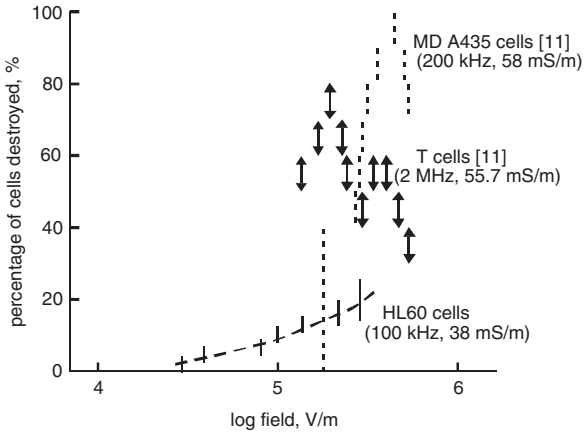

Fig. 6 *Results extracted from [11] on the electromediated bursting of T cells and breast cancer cells (MDA-MB-435) are shown with our cell bursting data for HL60 cells. The conductivities of the suspending media are given, and the AC frequency values cited correspond to those where cell bursting was most probable for each cell type*

respectively. The average cell radius was taken as 5.2 μm [20], to give $\tau = 9.5 \times 10^{-7}$ s for the time constant of the T cells. For the HL60 cells the value for C_m was obtained from measurement of the cross-over frequency f_{xo} for 90 cells that did not burst. Observed values for f_{xo} ranged from 57–93 kHz, and gave an average value close to 75 kHz. The radii of the HL60 cells were determined to range from 6.0–7.5 μm (± 0.25 μm) with an average value close to 6.75 μm. This gives a C_m value of 17.8 mF/m^2 for the HL60 cells, and a corresponding time constant value $\tau = 1.66 \times 10^{-6}$ s.

The average radii and time constant values (5.2 μm, 9.5×10^{-7} s; 6.75 μm, 1.66×10^{-6} s, for the T and HL60 cells, respectively) were used in (4) to create the curves drawn in Fig. 5 to show how the membrane field generated parallel to the applied field varies as a function of frequency. These curves are plotted in Fig. 5 for values of external field of 30 and 40 kV/m for the HL60 and T cells, respectively. The cross-over frequency ranges, where cells exhibited a change from negative to positive DEP with increasing frequency, are also shown in Fig. 5 for the HL60 cells ($f_{xo} \sim 60$–90 kHz) and T cells ($f_{xo} \sim 110$–190 kHz).

5 Discussions and conclusions

The data shown in Fig. 4 indicate that in our DEP experiments a small number ($\sim 5\%$) of cells in suspension were induced to burst if they were directed by positive DEP towards regions at the electrode edges where the local sinusoidal fields exceeded a value of about 30 kV/m. For cells suspended in an isotonic electrolyte of conductivity 40 mS/m and with applied AC voltages between 1 and 6 V (pk), very few cell bursting events were observed in the frequency range from 10 kHz up to the cross-over frequency f_{xo} where the cells made the transition from negative to positive DEP. We assume that in this lower frequency range the cells were directed away from the electrode edges and were never subjected to field stresses greater than 30 kV/m.

From Fig. 5 the critical membrane field for the onset of cell destruction for both the HL60 and T cells is of the order of 10^8 V/m for frequencies just slightly above their respective f_{xo} cross-over frequencies, and progressively drops (to a value of the order of 10^7 V/m for T cells) as the frequency is raised above f_{xo}. This suggests that a combination of stresses induced by both the increase of the membrane field stress and the DEP force acting on the cell leads to cell

destruction. At frequencies just above the cross-over frequency f_{xo} it is common in DEP experiments to observe cells spinning at electrode edges under the influence of an induced rotational torque. Such behaviour can result in significant shear forces on the cell membrane, resulting in cell damage [1]. Above a certain frequency, however, where the membrane field falls below 10^7 V/m, the DEP force acting alone is not sufficient to initiate cell destruction. A previous report [11] has described unpublished work to show that different cell types have characteristically different susceptibilities to destruction by AC fields. Although the experimental details of this earlier work are not provided, some interesting comparisons can be made with our work presented here. As shown in Fig. 6, T cells and breast cancer cells subjected to an AC field exhibited maximum cell damage at frequencies around 2 MHz and 200 kHz, respectively [11]. This mirrors the different field-frequency windows for cell destruction of HL60 and T cells shown in Figs. 4 and 5, and suggests that in this earlier work [11] the applied fields were not uniform and that DEP forces could have contributed to the overall stresses acting on the cells. However, as shown in Fig. 6, the number of cell bursting events was much higher than for our DEP work, with 40–100% of the total cells typically being destroyed. This suggests that finer control of electromediated cell bursting can be achieved using DEP fields generated by microelectrode arrays, especially if they are specifically designed to create very localised high field regions. Also, as shown in Fig. 6, in the earlier work [11] the cell bursting probability reached a peak value and then decreased with increasing applied voltage. Without the experimental details it is difficult to understand the reason for this effect, but a possible cause could be an increase of the surrounding medium conductivity as a result of the release of cytoplasm electrolyte from the large number of bursting cells.

As a general guide, it appears that to minimise cell destruction the possibility of cells being exposed to fields above 30–40 kV/m should be avoided, especially in the half-decade frequency range immediately above the DEP cross-over frequency where the induced membrane field has yet to fall off significantly in magnitude. Minimising cell damage could be achieved by 'masking' the electrode regions marked 'A' and 'B' in Fig. 1 with an insulating oxide or polymer film, for example. The location of this frequency window, for a fixed medium conductivity, is defined by the size, morphology (i.e. C_m value) and dielectric properties of a cell type. So, alternatively, this field-frequency window can be exploited to selectively destroy specific cell types in a cell mixture. For example, for a mixture of HL60 and Jurkat T cells, either the HL60 or T cells could be selectively destroyed by applying large AC signals at a frequency of either 100 kHz or 1 MHz, respectively.

The work reported here employed cell suspending media of conductivity near 40 mS/m, but inspection of (5) and (6) indicates that our conclusions will also hold for other values of the medium conductivity. For intact cell membranes, the membrane conductivity σ_m is so small that (5) can to a good approximation be given as:

$$\tau \approx \frac{RC_m(\sigma_i + 2\sigma_e)}{2\sigma_i\sigma_e} \tag{7}$$

If we define $f_{mf} = 1/(2\pi\tau)$ as the frequency where the absolute value of the induced membrane field falls off by a factor of $1/\sqrt{2}$ from its maximum value given by (4), then on substituting for C_m in (5) and (6) we obtain from (7) the result:

$$f_{xo} = \frac{f_{mf}}{\sqrt{2}}\left(1 + \frac{2\sigma_e}{\sigma_i}\right) \tag{8}$$

Equation (8) teaches that the close relationships between the DEP cross-over frequency and the fall in membrane fields shown in Fig. 5 can be expected to hold for the range (1–200 mS/m) of medium conductivities commonly employed in DEP experiments on cells.

6 Acknowledgments

We thank Dr Sally Cotterill and Brenda Kusler for their work with cell cultures, and Drs Mark Talary and Richard Lee for their help with the dielectrophoresis experiments. Part of this work was funded by the National Foundation for Cancer Research.

7 References

1 Pethig, R., Talary, M.S., and Lee, R.S.: 'Enhancing traveling-wave dielectrophoresis with signal superposition', *IEEE Eng. Med. Biol. Mag.*, 2003, **22**, (6), pp. 43–50
2 Becker, F.F., Wang, X.B., Huang, Y., Pethig, R., Vykoukal, J., and Gascoyne, P.R.C.: 'The removal of human leukaemia cells from blood using interdigitated microelectrodes', *J. Phys. D, Appl. Phys.*, 1994, **27**, pp. 2659–2662
3 Stephens, M., Talary, M.S., Pethig, R., Burnett, A.K., and Mills, K.I.: 'The dielectrophoresis enrichment of $CD34^+$ cells from peripheral stem cell harvests', *Bone Marrow Transplant*, 1996, **18**, pp. 777–782
4 Fuhr, G., Glasser, H., Müller, T., and Schnelle, T.: 'Cell manipulation and cultivation under a.c. electric field influence in highly conductive culture media', *Biochim. Biophys. Acta*, 1994, **1201**, (3), pp. 353–360
5 Huang, Y., Joo, S., Duhon, M., Heller, M., Wallace, B., and Xu, X.: 'Dielectrophoretic cell separation and gene expression profiling on microelectronic chip arrays', *Anal. Chem.*, 2002, **74**, (14), pp. 3362–3371
6 Markx, G.H., and Pethig, R.: 'Dielectrophoretic separation of cells: Continuous separation', *Biotechnol. Bioeng*, 1995, **45**, pp. 337–343
7 Leverett, L.B., Hellums, L.D., Alfrey, C.P., and Lynch, E.C.: 'Red blood cell damage by shear stress', *Biophys. J.*, 1972, **12**, pp. 257–273
8 Chittur, K.K., McIntire, L.V., and Rich, R.R.: 'Shear stress effects on human T cell function', *Biotechnol. Prog.*, 1988, **4**, (1), pp. 89–93
9 Gascoyne, P.R.C., Pethig, R., Burt, J.P.H., and Becker, F.F.: 'Membrane changes accompanying the induced differentiation of Friend murine erythroleukemia cells studied by dielectrophoreis', *Biochim. Biophys. Acta*, 1993, **1149**, (1), pp. 119–126
10 Neumann, E., Sowers, A.E. and Jordan, C.A. (Eds.).: 'Electroporation and electrofusion in cell biology' (Plenum Press, New York, 1989)
11 Gascoyne, P.R., and Vykoukal, J.V.: 'Dielectrophoresis-based sample handling in general-purpose programmable diagnostic instruments', *Proc. IEEE*, 2004, **92**, (1), pp. 22–42
12 Panofsky, W.K.H., and Phillips, M.: 'Classical electricity and magnetism' (Addison-Wesley, Reading, MA, 1955)
13 Pohl, H.A.: 'Dielectrophoresis' (Cambridge University Press, Cambridge, 1978)
14 Debye, P.: 'Polar molecules' (Chemical Catalog Co., New York, 1929)
15 Sauer, F.A.: 'Interaction forces between microscopic particles in an external electromagnetic field', in Chiabrera, A., Nicolini, C. and Schwan, H.P. (Eds.).: 'Interactions between electromagnetic fields and cells' (Plenum, New York, 1985), pp. 181–202
16 Jones, T.B.: 'Electromechanics of particles' (Cambridge University Press, Cambridge, 1995)
17 Pethig, R., and Markx, G.H.: 'Applications of dielectrophoresis in biotechnology', *Tibtech*, 1997, **15**, (10), pp. 426–432
18 Kotnik, T., Bobabovic, F., and Miklavcic, D.: 'Sensitivity of transmembrane voltage induced by applied electric fields—a theoretical analysis', *Bioelectrochem. Bioenergetics*, 1997, **43**, pp. 285–291
19 Kotnik, T., and Miklavcic, D.: 'Second-order model of membrane electric field induced by alternating external electric fields', *IEEE Trans. Biomed. Eng.*, 2000, **47**, (8), pp. 1074–1081
20 Pethig, R., Bressler, V., and Carswell-Crumpton, C. *et al.*: 'Dielectrophoretic studies of the activation of human T lymphocytes using a newly developed cell profiling system', *Electrophoresis*, 2002, **23**, (13), pp. 2057–2063
21 Price, J.A.R., Burt, J.P.H., and Pethig, R.: 'Applications of a new optical technique for measuring the dielectrophoretic behaviour of microorganisms', *Biochim. Biophys. Acta*, 1988, **964**, (2), pp. 221–230
22 Huang, Y., and Pethig, R.: 'Electrode design for negative dielectrophoresis', *Meas. Sci. Technol.*, 1991, **2**, (12), pp. 1142–1146